Hadronic Correlation Functions in the QCD Plasma Phase

K. D. Born,[1] Sourendu Gupta,[2] A. Irbäck,[2] F. Karsch,[3,4] E. Laermann,[4] B. Petersson,[3] and H. Satz[2,3]

(The MT$_c$ Collaboration)

[1]*Institute for Theoretical Physics E, Rheinisch-Westfälische Technische Hochschule Aachen, D-5100 Aachen, Federal Republic of Germany*
[2]*Theory Division, CERN, CH-1211, Geneva 23, Switzerland*
[3]*Fakultät für Physik, Universität Bielefeld, D-4800 Bielefeld 1, Federal Republic of Germany*
[4]*Hochstleistungsrechenzentrum, Kernforschungsanlage Jülich, D-5170 Jülich, Federal Republic of Germany*
(Received 4 April 1991)

We present results for static hadronic correlation functions in the high-temperature phase of QCD with four flavors of dynamical quarks. We confirm chiral-symmetry restoration through the degeneracies of the spectrum of screening lengths. We also find that the screening lengths for the ρ and N channels at $T \gtrsim 1.2T_c$ are close to that in a free quark gas.

PACS numbers: 12.38.Gc, 12.38.Mh

Simulations of lattice QCD have shown that chiral symmetry is restored at high temperatures, as indicated by the vanishing of the chiral order parameter $\langle\bar{\chi}\chi\rangle$ [1]. Additional evidence for the restoration of chiral symmetry can be obtained by using hadronic correlation functions, first studied by DeTar and Kogut [2]. The exponential falloff of such correlations at large spatial separations determines screening lengths, and unbroken symmetries are reflected in degeneracies of these screening lengths. Hadronic correlation functions also yield information on the real-time modes of the high-temperature phase. If the plasma phase contains hadronic modes, as argued by DeTar and Kogut [2], then the corresponding correlation functions should be screened. On the other hand, free quarks also lead to screening in the imaginary-time formulation—through the existence of a finite infrared cutoff on the Euclidean-time components of momenta. It is therefore important to determine the temperature dependence of these screening lengths and to compare them with the results of a computation with free quarks.

In this Letter we present results for hadronic correlations obtained on an 8×16^3 lattice with four flavors of dynamical quarks of mass $m_q a = 0.01$, and compare them to values obtained for a gas of free quarks, taking into account finite-size effects in the latter case. We performed measurements on configurations generated by the MT$_c$ Collaboration with the hybrid Monte Carlo algorithm (see Ref. [3] for details of the runs), using approximately twenty configurations at each β, separated by about fifty trajectories, in order to take care of autocorrelations. At $\beta = 5.15$ (our estimate for β_c), where two runs from different starts indicated the presence of metastabilities, we made separate analyses for the two.

We restrict our analysis to spatial correlations between local hadronic operators constructed from staggered fermions. The construction of static correlation functions uses methods familiar from mass spectrum analysis at zero temperature [4]. We use a notation common for the corresponding zero-temperature correlations: M_{PS}, M_{SC}, M_{VT}, and M_{PV} for the meson correlations and B for the baryon correlation [5]. We measured correlations in the z direction. To compensate for antiperiodicity in the imaginary-time direction τ, we replaced the temporal average in B by

$$B(z) = \sum_{x,y,\tau} \cos(\omega_0 \tau) B(x,y,z,\tau), \tag{1}$$

where $\omega_0 = \pi T$ is the lowest Matsubara frequency.

It is possible to test for chiral-symmetry restoration directly from the correlation functions without extracting screening masses. Following Ref. [6], we construct for this purpose the chiral projections

$$M_0^{\pm}(z) = M_{PS}(z) \pm (-1)^z M_{SC}(z) = \sum_{x,y,\tau} |G_{0,r}|^2 [1 \pm (-1)^{x+y+z+\tau}]. \tag{2}$$

Here $G_{0,r}$ is the quark propagator and the factor $1 \pm (-1)^{x+y+z+\tau}$ is the equivalent of $1 \pm \gamma_5$ for staggered fermions. The vanishing of one of these projections, in the limit of massless quarks, implies parity doubling of masses of states that contribute to the correlation function. On the other hand, if these states are not degenerate, then the ratio M_0^+/M_0^- should tend to 1 at large separation. Our results for M_0^+/M_0^- are shown in Fig. 1. Although the ratio is nonzero at all couplings, due to the finite quark mass, the clear difference in behavior between correlators at high and low temperatures suggests a restoration of chiral symmetry at β_c. It is especially instructive to compare results for the two metastable branches at T_c with zero-temperature simulations on 24×16^3 lattices, which have been performed with the same quark mass and at the same coupling ($\beta = 5.15$). The correlation functions for the $T = 0$ simulations and the branch corresponding to the chiral-symmetry-broken phase at T_c are in good agreement, whereas that for the

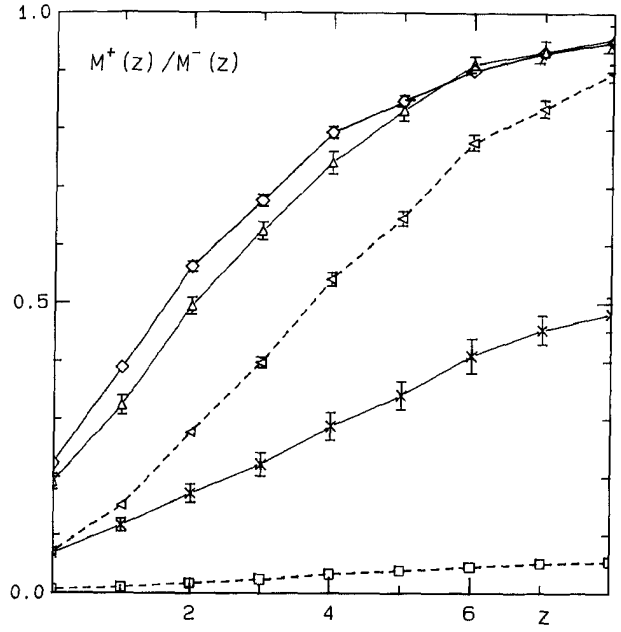

FIG. 1. Comparison of $M_0^+(z)/M_0^-(z)$ for quark mass $m_q a = 0.01$ on finite- and zero-temperature lattices. Shown are results for coupling $\beta = 5.15$ on an 8×16^3 lattice from the chiral-symmetry-broken (triangles) and symmetric (crosses) phases together with zero-temperature data obtained on a 24×16^3 lattice (diamonds). The dashed lines show results at $\beta = 5.3$ (squares) for lattice size 8×16^3, which should be compared with those at $\beta = 5.35$ (inverted triangles) for lattice size 24×16^3.

chiral-symmetric branch at T_c is significantly smaller. We also find that the finite-temperature result at $\beta = 5.3$ is much smaller even than that obtained at $T = 0$ for $\beta = 5.35$, as shown by the dashed curves in Fig. 1.

In order to compare our results for the screening masses with those for a free quark gas, we consider finite-size effects in some detail. Although this consideration may seem quite technical, it is of particular importance as it constitutes the basis for our conclusions, which differ from those of Refs. [2] and [7]. On a $N_\tau \times N_s^2 \times \infty$ lattice (where the z direction is infinite), the pseudoscalar correlation function for $m_q = 0$ takes the form

$$M_{PS}(z) = \frac{2^3}{N_\tau N_s^2} \sum_{k_1,k_2,k_4} \frac{1}{1+\tilde{\omega}^2} \exp(-2\hat{\omega}|z|), \quad (3)$$

with

$$\tilde{\omega}^2 = \sin^2\left(\frac{2\pi k_1}{N_s}\right) + \sin^2\left(\frac{2\pi k_2}{N_s}\right) + \sin^2\left(\frac{2\pi k_4}{N_\tau}\right),$$
$$\hat{\omega} = \ln[\tilde{\omega} + (1+\tilde{\omega}^2)^{1/2}]. \quad (4)$$

The momentum sum runs over $k_1, k_2 = 1, 2, \ldots, N_s/2$ and $k_4 = 1/2, 3/2, \ldots, N_\tau/2 - 1/2$. From this expression we see explicitly that the lowest possible frequency $\hat{\omega}$ is nonvanishing, due to the antiperiodicity in the transverse imaginary-time direction. The correlation function thus falls off exponentially at large separations z, even when the quark mass is zero. The finite temporal extent N_τ of the lattice leads to a shift of the lowest Matsubara frequency from the continuum value $\omega_0 = \pi T$ to a value $\hat{\omega}_0$ given by Eq. (4). For $N_\tau = 4$ we have $\hat{\omega}_0 = 2.634T$, corresponding to a shift of 16%; for $N_\tau = 8$ the shift is 4.8%.

In our calculations on $N_\tau \times N_s^3$ lattices, we must also account for the finite extent of the lattice in the z direction. For moderate values of N_s this effect turns out to be more important than the shift of ω_0 induced by the finite temporal extent of the lattice (N_τ). In order to quantitatively estimate this effect, we consider an effective screening mass $\mu(z)$ evaluated at a distance $z = N_s/4$ from the ratios $M_{PS}(z-1)/M_{PS}(z+1)$ of the correlation functions. These correlation functions have been calculated from an explicit momentum sum on $N_\tau \times N_\sigma^3$ lattices similar to that in Eq. (3) [8]. In Fig. 2 we show $\mu(z)$ for $N_\tau = 4$ and 8 and various values of N_s. For $N_s = 16$ finite-size effects are large, especially for $N_\tau = 8$. Hence, in comparing measurements of screening masses with the free case, we have used the result shown in Fig. 2, which are the same for all meson channels, and the corresponding one for the baryon correlation function. Note that we calculate mesonic screening masses only for even z; for odd z, predictions for the different meson channels differ by $O(m_q^2)$ corrections.

We extract the lowest screening masses μ by fitting the correlation functions to a sum of one oscillating and one monotonic term. We fitted data folded to the interval $0 \le z \le N_s/2$, and use only the correlations for $z \ge z_{min}$,

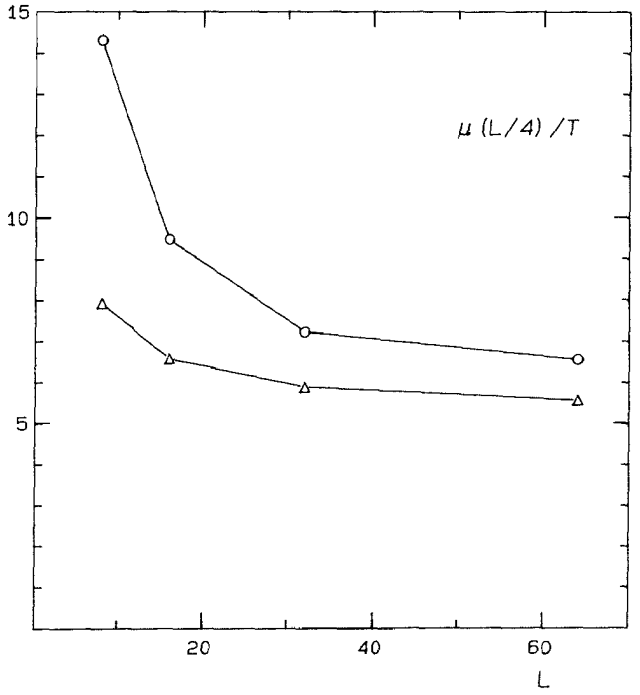

FIG. 2. Effective screening mass $\mu(z)$ for the free form of the correlation function $M_{PS}(z)$ as a function of the spatial lattice size N_s. Circles are for $N_\tau = 8$, triangles for $N_\tau = 4$. Both for $N_\tau = 4$ and 8 we used $m_q/T = 0.08$. The effects of the nonzero quark mass are small.

choosing $z_{\min}$ to be always greater than 1. For M_{PS} and $(-1)^z M_{SC}$ we found no significant contribution from an oscillating component, and final numbers μ_π and μ_σ have been obtained by two-parameter fits. We employed correlated χ^2 fits [9] in order to obtain reasonable estimates of errors and goodness of fit.

Our results for the different screening lengths are collected in Fig. 3. These confirm the presence of a chiral-symmetry-restoring phase transition between $\beta=5.1$ and 5.2. We have sufficient statistics to extract the baryonic screening masses μ_N and $\mu_{N'}$ only at $\beta \geq 5.2$. There we find them to be equal, and it is the common value obtained from a four-parameter fit that is plotted. At these couplings we further found that $\mu_\pi \approx \mu_\sigma$ and $\mu_\rho \approx \mu_{A_1}$. Figure 3 also shows the zero-temperature masses m_π, m_ρ, and m_N at $\beta=5.15$, which have been taken from Ref. [10]. In the broken phase, the screening masses seem to be similar to their zero-temperature counterparts. Finally, we compare the screening masses at high temperatures with their free values, obtained in the way explained above. At our highest β value ($\beta=5.3$) the temperature is around $1.2T_c$. Already at this coupling we see that μ_ρ, μ_{A_1}, and μ_N differ by less than 10% from values which would correspond to free quark propagation in this quantum number channel. The scalar and pseudoscalar screening masses, μ_σ and μ_π, are, however, only about half the free-gas value in this temperature regime.

To check if the agreement with the free case found above was accidental, we also performed some calculations in the quenched approximation. Screening masses were determined on a 4×16^3 lattice for quark mass $m_q/T=0.08$. The results are displayed in Fig. 4. Note that in our determination of the phase-transition temperature for $N_f=4$ we found T_c/m_H values significantly smaller than those that have been obtained in quenched calculations [3]. At $T<T_c$, we might therefore expect that the dimensionless ratios μ/T are smaller in the quenched approximation than in the four-flavor case studied above. The data in Figs. 3 and 4 seem consistent with such a flavor dependence. Apart from this, the results above T_c are similar in the two cases. For $T_c \leq T \leq 1.5T_c$, both sets of screening masses change rapidly from the low-temperature values to those that correspond to free quark propagation on finite lattices. As can be deduced from Fig. 2, the asymptotic results for free quark propagation differ for this lattice size by more than 50% from the corresponding results on an 8×16^3 lattice. The fact that the Monte Carlo data correctly reproduce the finite lattice artifacts (although they are quite different for these two lattice sizes) indicates that the agreement with the free case persists in the large-volume limit. The quenched calculations were also extended to higher temperatures. Above $T=1.5T_c$, we found that μ/T ratios are only weakly T dependent.

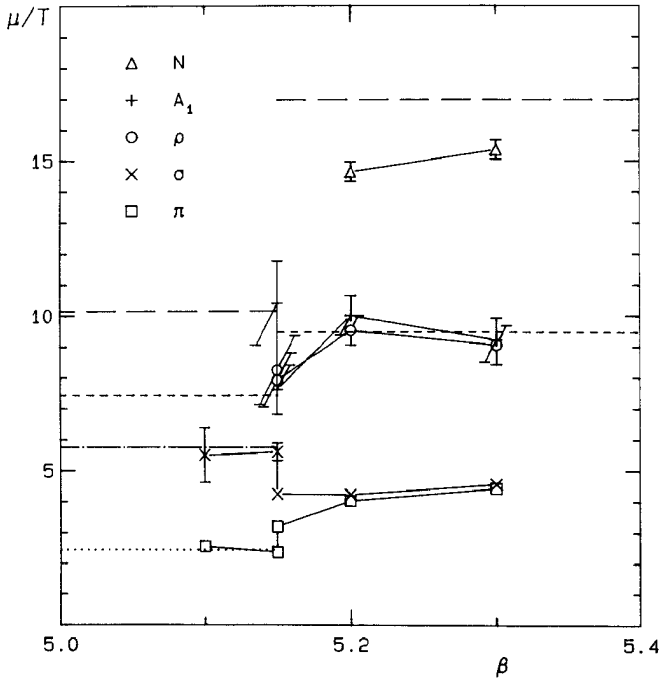

FIG. 3. Screening masses μ/T as a function of β for $N_f=4$ from an 8×16^3 lattice. Lines on the left-hand side give the values of the zero-temperature masses in units of T_c: m_π/T_c (dotted line), m_σ/T_c (dash-dotted line), m_ρ/T_c (short-dashed line), and m_N/T_c (long-dashed line) obtained at $\beta=5.15$. Lines on the right-hand side give the values for screening masses corresponding to free quark propagation in the mesonic (short-dashed line) and baryonic (long-dashed line) channels.

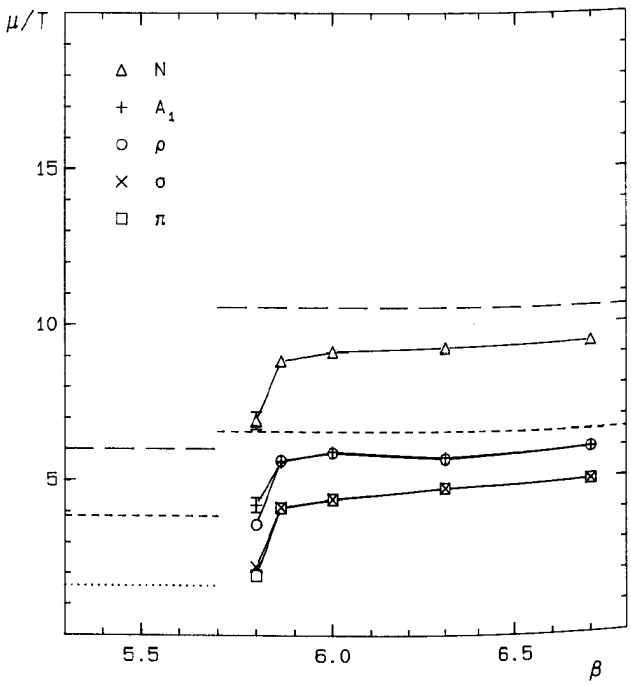

FIG. 4. Same as Fig. 3 but for the quenched case on a 4×16^3 lattice. The data at $\beta=5.865$, which corresponds to $T=1.5T_c$, are from Ref. [7]. The zero-temperature hadron masses were obtained at $\beta=5.7$ in Ref. [12]. Note the difference in the values for free quark propagation in comparison to Fig. 3, which is entirely due to the different lattice sizes used.

Summarizing, we have presented results for hadronic screening lengths in four-flavor QCD at high temperatures. The results confirm the existence of a chiral-symmetry-restoring phase transition and are in complete agreement with our earlier conclusions from measurements of $\langle\bar{\chi}\chi\rangle$ [3]. We have compared the extracted screening masses with values for a gas of free quarks. The π and σ masses approach the free-quark-gas values slowly, whereas already at temperature $T \approx 1.2T_c$ we find that screening masses corresponding to the spin-one meson and the baryon channels are close to the values for free quarks. This suggests that the states in these channels propagate in the plasma as weakly interacting quarks rather than as deeply bound states. This conclusion furthermore removes the paradox between the results for screening masses and the baryon-number susceptibility. The value of the latter quantity in the high-temperature phase signals the presence of light states in the plasma [11]. Although our results should be confirmed by extending the spatial size of the lattice, the quenched computation leads us to believe that finite-size effects do not influence them qualitatively at this moderate value of the temperature. The nonperturbative effects seen in the π channel deserve further investigations. We are currently studying the dispersion relations in this channel in more detail.

The numerical work described was performed on the CRAY-YMP computer at HLRZ, Jülich. Financial support from Deutsche Forschungsgemeinschaft under Contract No. Pe 340/1-3 and the Ministerium für Wissenschaft und Forschung NRW under Contract No. IVA5-10600990 is gratefully acknowledged.

[1] For a recent review, see A. Ukawa, Nucl. Phys. B (Proc. Suppl.) **17**, 118 (1990).

[2] C. DeTar and J. Kogut, Phys. Rev. Lett. **59**, 399 (1987); Phys. Rev. D **36**, 2828 (1987).

[3] R. V. Gavai, S. Gupta, A. Irbäck, F. Karsch, S. Meyer, B. Petersson, H. Satz, and H. W. Wyld, Phys. Lett. B **241**, 567 (1990).

[4] H. Kluberg-Stern, A. Morel, O. Napoly, and B. Petersson, Nucl. Phys. **B220**, 447 (1983); M. Golterman, Nucl. Phys. **B273**, 663 (1986).

[5] K. C. Bowler, C. B. Chalmers, R. D. Kenway, G. S. Pawley, and D. Roweth, Nucl. Phys. **B284**, 299 (1987).

[6] S. Gottlieb, W. Liu, D. Toussaint, R. L. Renken, and R. L. Sugar, Phys. Rev. Lett. **59**, 1881 (1987).

[7] A. Gocksch, P. Rossi, and U. M. Heller, Phys. Lett. B **205**, 334 (1988).

[8] The explicit momentum sums for propagators on finite lattices are somewhat lengthy in the case of staggered fermions. They will be published elsewhere.

[9] T. A. DeGrand and C. E. DeTar, Phys. Rev. D **34**, 2469 (1986); S. Gottlieb, W. Liu, R. L. Renken, R. L. Sugar, and D. Toussaint, Phys. Rev. D **38**, 2245 (1988).

[10] E. Laermann, R. Altmeyer, K. D. Born, M. Göckeler, R. Horsely, W. Ibes, T. F. Walsh, and P. M. Zerwas, in Proceedings of Lattice '90 [HLRZ Report No. HLRZ-90-98 (to be published)].

[11] S. Gottlieb, W. Liu, D. Toussaint, R. L. Renken, and R. L. Sugar, Phys. Rev. Lett. **59**, 2247 (1987).

[12] APE Collaboration, P. Bacilieri *et al.*, Nucl. Phys. **B343**, 228 (1990).